Manganese as a Replacement for Magnesium and Zinc: Functional Comparison of the Divalent Ions

Charles W. Bock,[†,‡] Amy Kaufman Katz,[†] George D. Markham,[†] and Jenny P. Glusker*[,†]

Contribution from The Institute for Cancer Research, Fox Chase Cancer Center, Philadelphia, Pennsylvania 19111, and Philadelphia University, Philadelphia, Pennsylvania 19144

Received March 3, 1999. Revised Manuscript Received June 18, 1999

Abstract: Divalent manganese, magnesium, and zinc fill unique roles in biological systems, despite many apparently similar chemical properties. A comparison of the liganding properties of divalent manganese, magnesium, and zinc has been made on the basis of data on crystal structures (from the Cambridge Structural Database and the Protein Databank) and molecular orbital and density functional calculations. The distribution of coordination numbers for divalent manganese in crystal structure determinations, and the identities of ligands, have been determined from analyses of data derived from the structural databases. Enthalpy and free energy changes for processes such as loss of water or ionization of water from hydrated cations have been evaluated from computational studies. The energy penalty for changing the hexahydrate of divalent manganese to a pentahydrate with one water molecule in the second coordination shell is intermediate between the high value for magnesium and the low value for zinc. The preferred coordination number of divalent manganese is six, as it is for magnesium, while the preferred coordination is less definite for zinc and ranges from 4 to 6. Magnesium generally binds to oxygen ligands, and divalent manganese behaves similarly, although it is more receptive of nitrogen ligands, while zinc prefers nitrogen and sulfur, especially if the coordination number is low. The slightly lower discrimination between nitrogen and oxygen of divalent manganese, compared to magnesium, was apparent both in the energetics of competition of these cations for water and ammonia and from ligand binding profiles in the crystallographic databases.

Introduction

The element manganese is widely distributed in nature. Of the first-row transition metals, manganese is second only to iron in terms of its natural abundance.[1−3] Manganese is found in minerals mainly as an oxide or as a carbonate. It is therefore not surprising that a wide variety of plant and animal life forms have evolved with a critical requirement for manganese as a trace element.[1] This reflects not only its high relative abundance and accessibility but also the versatility of its coordination chemistry, together with its wide range of oxidation states (from −III to +VII).[3] As noted by Williams and da Silva,[1] manganese has two major functions in enzymes: (1) as a Lewis acid, for which its properties can be compared with those of magnesium, zinc, and calcium, and (2) as an oxidation catalyst, for which it can be compared with iron and copper. The first of these two functions involves divalent manganese, which is the subject of studies reported here. We present an analysis of ligand binding to divalent manganese, some of its chemical and stereochemical properties relevant to biological systems, and a comparison with the properties of divalent magnesium and zinc.

Divalent manganese has a radius of approximately 0.75 Å, somewhat larger than that of magnesium (0.65 Å), smaller than that of calcium (0.99 Å), and almost the same as that of zinc (0.74 Å).[4,5] In view of the similar sizes and charges of divalent manganese and zinc, they might be expected to substitute for each other readily in biochemical reactions. This, however, is generally not the case; the chemical and biochemical behavior of divalent manganese resembles that of magnesium more than zinc. The major difference between magnesium and manganese involves their available oxidation states (II for magnesium, many for manganese). Divalent manganese is the most stable oxidation state of manganese in acid and neutral aqueous solutions. In alkaline solutions, however, the hydroxide forms and is readily oxidized.

It has been shown experimentally that when divalent manganese replaces magnesium in the active site of a magnesium-utilizing enzyme, the catalytic activity of that enzyme often is maintained.[6] This observation has led to the widespread use of manganese as a spectroscopically active replacement for magnesium,[7] because, unlike magnesium, it is paramagnetic.[8] Magnesium, however, is less often a catalytically competent replacement for divalent manganese in enzymes because the role of manganese in some enzymes is unique, and it apparently cannot be replaced by other metal ions for reasons that are as

* Address correspondence to Jenny P. Glusker, The Institute for Cancer Research, Fox Chase Cancer Center, 7701 Burholme Ave., Philadelphia, PA 19111. Tel.: 215-728-2220. Fax: 215-728-2863. E-mail: jp_glusker@fccc.edu.

† Fox Chase Cancer Center.

‡ Philadelphia University.

(1) Fraústo da Silva, J. J. R.; Williams, R. J. P. *The Biological Chemistry of the Elements. The Inorganic Chemistry of Life*; Clarendon Press: Oxford, England, 1991.

(2) Christianson, D. W. *Prog. Biophys. Mol. Biol.* **1997**, *67*, 217−252.

(3) Cotton, F. A.; Wilkinson, G. *Advanced Inorganic Chemistry. A Comprehensive Text*, 4th ed.; John Wiley and Sons: New York, 1980.

(4) Brown, I. D. *Acta Crystallogr.* **1988**, *B44*, 545−553.

(5) Glusker, J. P. *Adv. Protein Chem.* **1991**, *42*, 1−73.

(6) Schramm, V. L., Wedler, F. C., Eds. *Manganese in Metabolism and Enzyme Function*; Academic Press: New York, 1986.

(7) Mildvan, A. S. In *The Enzymes*; Boyer, P. D., Ed.; Academic Press: New York, 1970; Vol. 2, pp 446−536.

(8) Reed, G. H.; Markham, G. D. *Biol. Magn. Reson.* **1986**, *6*, 73−142.

10.1021/ja9906960 CCC: $18.00
Published on Web 08/03/1999

yet unclear.[7] We have investigated here the similarities in coordination of magnesium and divalent manganese, and we show that cations of the two elements behave remarkably similarly. Furthermore, comparisons show that zinc behaves quite differently from magnesium and manganese with respect to its preferred coordination number and the type of ligand it prefers (its "binding profile").

Methods

A. Structural Analyses of Ligand-Bound Metal Ions. The coordination geometries of Mn^{2+}, Mg^{2+}, and Zn^{2+} ions were probed using atomic coordinates of the crystal structures containing these cations in the Cambridge Structural Database (CSD, 1998 versions).[9] In addition, molecular orbital and density functional studies of some simple complexes of these cations were carried out to investigate the energetic consequences of dehydration, deprotonation, and proton transfer. The work described here concentrates on Mn^{2+}, and the published results for Mg^{2+} and Zn^{2+} are used for comparisons.[10−14]

The CSD was searched for all published crystal structures of Mn^{2+} ions by use of the program Quest3D that is connected with this database. A master file was created of three-dimensional coordinates and bibliographic references of crystal structures found by this search. In addition, our data on the coordination geometries and binding preferences of magnesium (published in 1994)[10] were updated by a new analysis. Only those crystal structures with divalent manganese, magnesium, or zinc bound to the elements O, N, Cl, Br, and/or S were considered, because we are interested in cation interactions in biological systems. Some crystal structures were eliminated from the search because they contained disorder and/or the crystallographic *R* factor was high (greater than 0.10).

The master file so obtained was then broken down into files for each individual specific coordination number (from 3 to 8). The coordination number of the metal ion in many crystal structures was evaluated by inspection of its surroundings in the crystal structure using the computer graphics program ICRVIEW.[15] In other crystal structures, the metal ion coordination number was evident from the chemical formula drawn by the software provided within the CSD program system. For viewing macromolecular crystal structures, the Protein Data Bank (PDB, 1998)[16] was accessed by way of the World Wide Web, and atomic coordinates were downloaded. The molecular structure was viewed by use of the graphics programs RASMOL[17] and ICRVIEW,[15] and the metal−ion coordination was evaluated for each structure.

B. Energetics of Reactions Involving Metal Ions. The energetics of dehydration, deprotonation, and proton-transfer reactions in the presence of divalent manganese were evaluated by ab initio molecular orbital and density functional theory calculations. These studies were aimed at examining the affinity of Mn^{2+} for water or other ligands and its ability to facilitate the ionization of water to give a metal ion−hydroxide complex. The GAUSSIAN 94 series of programs[18] were used, and calculations were carried out on CRAY computers at the National Cancer Institute (Frederick, MD), as well as Silicon Graphics and DEC alpha computers. Optimizations were performed in *all* cases at the Hartree−Fock (HF) level using a Huzinaga[19] <5,3,3,2,1;5,3;4,1> basis set for manganese augmented with an additional *p*-type polarization function ($\alpha_p = 0.092$) and the 6-31G* basis set for oxygen and hydrogen (HUZ*);[20] this basis set was chosen for computational efficiency in view of the large number of electrons and the open-shell nature of the Mn^{2+} species. In a few cases, the internally stored 6-311++G** basis set (which includes diffuse functions on all the atoms) was employed so that direct comparisons with calculations on the corresponding magnesium complexes could be made. In selected cases, optimizations were also performed using second-order Møller−Plesset (MP2) perturbation theory[21] or density functional theory (DFT) using the B3LYP method[22−24] to incorporate the effects of electron correlation into the calculated geometry. The default convergence criteria in GAUSSIAN 94 were used.[18] Vibrational frequencies were obtained from analytical second derivatives calculated at the HF/HUZ*//HF/HUZ* level in order to verify that each calculated structure reported here corresponded to a local minimum on the potential energy surface (PES) at that level, and to estimate the thermal and entropic corrections required to obtain reaction enthalpies and free energies at 298 K.[25,26] For a number of the manganese complexes we considered, vibrational frequencies were obtained at higher computational levels, but this did not prove practical for general use, and HF/HUZ* frequencies were used throughout for consistency. Unless otherwise noted, no symmetry constraints were imposed during the optimizations. Numerous single-point calculations at the MP2(FULL)/HUZ* and MP2(FULL)/6-311++G** levels with all orbitals active (FULL)[18] were carried out at the HF/HUZ* geometries in order to evaluate reaction energies more precisely. Natural population analyses (NPAs) were performed using the SCF and MP2 densities to provide atomic charges and natural electron configurations.[27,28]

Results

I. Binding Motifs of Divalent Mg, Mn, Ca, and Zn in Small Molecules. Geometries of the coordination spheres of divalent manganese in crystal structures were investigated in order to address the issue of why manganese is such a good replacement for magnesium in the active sites of enzymes. The geometries of Mn^{2+}-containing complexes are derived from the 542 crystal structures obtained from the CSD, as described in the Methods section. This list, with REFCODEs, is given in Table 1S (Supporting Information). Average values of $M^{2+}\cdots O$ distances and $O\cdots M^{2+}\cdots O$ angles (M = Mn, Mg) for various experimentally observed manganese(II) and magnesium(II)[10] coordination numbers are given in Table 1. A comparison of the

(9) Allen, F. H.; Bellard, S.; Brice, M. D.; Cartwright, B. A.; Doubleday, A.; Higgs, H.; Hummelink, T.; Hummelink-Peters, G. G.; Kennard, O.; Motherwell, W. D. S.; Rodgers, J. R.; Watson, D. G. *Acta Crystallogr.* **1979**, *B35*, 2331−2339.

(10) Bock, C. W.; Kaufman, A.; Glusker, J. P. *Inorg. Chem.* **1994**, *33*, 419−427.

(11) Katz, A. K.; Glusker, J. P.; Markham, G. D.; Bock, C. W. *J. Phys. Chem. B* **1998**, *102*, 6342−6350.

(12) Markham, G. D.; Glusker, J. P.; Bock, C. L.; Trachtman, M.; Bock, C. W. *J. Phys. Chem.* **1996**, *100*, 3488−3497.

(13) Bock, C. W.; Kaufman, A.; Glusker, J. P. *J. Am. Chem. Soc.* **1995**, *117*, 3754−3765.

(14) Hartmann, M.; Clark, T.; van Eldik, R. *J. Am. Chem. Soc.* **1997**, *119*, 9, 7843−7850.

(15) Erlebacher, J.; Carrell, H. L. ICRVIEW−Graphics program for use on Silicon Graphics computers from The Institute for Cancer Research; Fox Chase Cancer Center, Philadelphia, PA, 1992.

(16) Bernstein, F. C.; Koetzle, T. F.; Williams, G. J. B.; Meyer, E. F. Jr.; Brice, M. D.; Rodgers, J. R.; Kennard, O.; Shimanouchi, T.; Tasumi, M. *J. Mol. Biol.* **1977**, *112*, 535−542.

(17) Sayle, R. RasMol v2.5. A molecular visualisation program; Glaxo Research and Development, Middlesex, UK, October 1994.

(18) Frisch, M. J.; Trucks, G. W.; Schlegel, H. B.; Gill, P. M. W.; Johnson, B. G.; Robb, M. A.; Cheeseman, J. R.; Keith, T. A.; Peterson, G. A.; Montgomery, J. A.; Raghavachari, K.; Al-Laham, M. A.; Zakrzewski, V. G.; Ortiz, J. V.; Foresman, J. B.; Cioslowski, J.; Stefanov, B. B.; Nanayakkara, A.; Challacombe, M.; Peng, C. Y.; Ayala, P. Y.; Chen, W.; Wong, M. W.; Andres, J. L.; Replogle, E. S.; Gomperts, R.; Martin, R. L.; Fox, D. J.; Binkley, J. S.; Defrees, D. J.; Baker, J.; Stewart, J. J. P.; Head-Gordon, M.; Pople, J. A. *GAUSSIAN 94*, Revision A.1; Gaussian Inc.: Pittsburgh, PA, 1995.

(19) Huzinaga, S.; Andzelm, J.; Klobukowski, M.; Radzio-Andzelm, E.; Sakai, Y.; Tazewaki, H. *Gaussian Basis Sets for Molecular Calculations; Physical Sciences Data*; Elsevier: New York, 1984; Vol. 16.

(20) Hariharan, P. C.; Pople, J. A. *Theor. Chim. Acta* **1973**, *28*, 213−222.

(21) Møller, C.; Plesset, M. S. *Phys. Rev.* **1934**, *46*, 618−622.

(22) Becke, A. D. *J. Chem. Phys.* **1993**, *98*, 5648−5652.

(23) Becke, A. D. *Phys. Rev.* **1988**, *A 38*, 3098−3100.

(24) Johnson, B. G.; Gill, M. W.; Pople, J. A. *J. Chem. Phys.* **1993**, *98*, 5612−5626.

(25) Schlegel, H. B.; Binkley, J. S.; Pople, J. A. *J. Chem. Phys.* **1984**, *80*, 1976−1981.

(26) Pople, J. A.; Krishnan, R.; Schlegel, H. B.; Binkley, J. S. *Int. J. Quantum Chem., Quantum Chem. Symp.* **1979**, *13*, 225−241.

(27) Reed, A. E.; Curtiss, L. A.; Weinhold, F. *Chem. Rev.* **1988**, *88*, 899−926.

(28) Reed, A. E.; Weinstock, R. B.; Weinhold, F. *J. Chem. Phys.* **1985**, *83*, 735−746.

Table 1. Average Mg^{2+}−O and Mn^{2+}−O Bond Lengths (Å) and Angles[a] (deg) from Crystal Structures in the CSD as a Function of Coordination Number

	$M^{2+}\cdots O$		$O\cdots M^{2+}\cdots O$	
CN	Mg	Mn	Mg	Mn
3				
4	1.96(2)	2.12(1)	110(9)	105(6)
5	2.02(3)	2.12(5)	93(9)	95(10)
6	2.073(3)	2.172(4)	90(1)	90(3)
7		2.25(6)		84(8)

[a] Includes all ligands (H_2O, carboxyl, carbonyl, or hydroxyl groups, for example). The standard deviations are in parentheses.

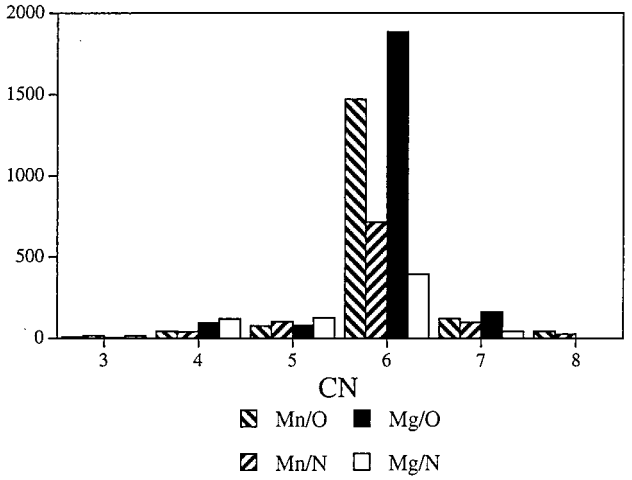

Figure 1. Binding preferences of divalent manganese and magnesium for oxygen and nitrogen. The number of entries in the CSD (vertical axis) for each coordination number (horizontal axis) is shown. The magnesium data are normalized (by a factor 2.0164) to give the same total number of entries as for manganese (see Table 2, 1586 entries for Mg^{2+}, 3198 entries for Mn^{2+}). Divalent manganese data are shaded, magnesium data are filled and unfilled.

binding of oxygen and nitrogen ligands by divalent manganese and magnesium is illustrated in Figure 1. The percentage of the various ligands (O, N, S, Cl, Br) for each coordination number is listed in Table 2 and shown for O and N in Figure 1, while the identities of the ligands around each manganese(II) ion are indicated in Table 3, with more details in Table 2S (Supporting Information).

Average $Mn^{2+}\cdots O$ distances are approximately 0.10 Å longer than those for $Mg^{2+}\cdots O$ (Table 1); this is consistent with the larger ionic radius of Mn^{2+} (0.75 Å) compared to that of Mg^{2+} (0.65 Å). On the other hand, the geometries of their octahedral structures are similar in that the average values for the $O\cdots M^{2+}\cdots O$ angles at coordination number 6 are 90.0°, although the standard deviation of the average angle is slightly lower for $O\cdots Mg^{2+}\cdots O$ than for $O\cdots Mn^{2+}\cdots O$, suggesting that Mn^{2+} may have a slightly more flexible coordination sphere than does Mg^{2+}.

There are striking similarities as well as some interesting differences between crystal structures containing divalent magnesium and those containing divalent manganese. The similarities, shown in Tables 2 and 3, are that both Mg^{2+} and Mn^{2+} generally bind six ligands (as was found in about 75% of the total number of structures for each), and oxygen is the most likely ligand for both, although less so for Mn^{2+} (77% for Mg, 61% for Mn). A major difference is that Mn^{2+}, as shown in Figure 1 and Table 2, more frequently binds nitrogen than does Mg^{2+}, especially at higher coordination numbers (i.e., 6−8). At the lower coordination number of 4, Mn^{2+} binds sulfur and chlorine more commonly than does Mg^{2+}, which still selects oxygen and nitrogen for binding. Therefore, Mg^{2+} can be considered harder than Mn^{2+}, implying that Mn^{2+} is slightly more polarizable, although the coordination number 6 is the most common to both.

These results can also be compared with those for zinc[13] and calcium,[29] obtained in the same way. It was found that 91% of bonds to Ca^{2+} in structures in the CSD involve oxygen. On the other hand, Zn^{2+} binds more frequently to nitrogen than does magnesium, especially at higher coordination numbers. These binding preferences are shown in Figure 2 by triangular plots of the average proportion of oxygen, nitrogen, and sulfur at each coordination number for Mn^{2+}, Mg^{2+}, Ca^{2+}, and Zn^{2+}. In these triangular plots, the percentage of O, N, S is represented up the height of the triangle (perpendicular to the base), with the vertex at 100%. We chose to indicate oxygen at the top vertex, nitrogen at the lower left vertex, and sulfur at the lower right vertex of these plots. The circles are filled for commonly found coordination numbers and open for the rarer coordination numbers. Nearly all entries cluster along the oxygen−nitrogen line, indicating the hardness of the metal ions and their low tendency to bind sulfur, which is softer. This is particularly marked for calcium, which mainly binds oxygen and occasionally nitrogen; no complexes with calcium liganded directly to sulfur have yet been reported in the CSD. Magnesium has ligand preferences similar to those of calcium for coordination numbers 6 and 7, but at low coordination numbers (3, 4, 5) it also binds nitrogen and, to a small extent, sulfur. The plot for divalent manganese is similar to that of magnesium but displaced toward nitrogen for coordination numbers 6−8 and toward sulfur for coordination number 4. In acceptance of nitrogen and sulfur ligands, divalent manganese is similar to zinc, except that the proportions of the various types of ligands are different; coordination number 4 is more common for Zn^{2+} than for Mn^{2+}. Based upon the structures present in the CSD, it appears that manganese is a good replacement for magnesium in sites with oxygen and nitrogen atoms available for liganding.

The tendencies of Mn^{2+} and Mg^{2+} to bind to water molecules and to carboxylate groups was also analyzed. We found that Mg^{2+} often binds to six water molecules; 41 structures out of 128 with six oxygen atoms around Mg^{2+} had six water molecules as ligands. Mn^{2+} commonly binds two water molecules and includes other functional groups in its inner coordination sphere. Mn^{2+} (unlike Mg^{2+}) also forms bidentate carboxylate complexes. The fraction of carboxyl ligands involving Mg^{2+}, Mn^{2+}, Ca^{2+}, and Zn^{2+} that are bidentate was examined as a function of coordination number (referred to as CN in the text that follows). It was found that Mg^{2+} has not been observed in a bidentate carboxylate complex and that Mn^{2+}, at CN = 5, also forms only monodentate carboxylate structures; however, at CN = 6, 3% of Mn^{2+} carboxyl ligands are bidentate, and this value increases to 15% at CN = 7. For Ca^{2+}, at CN = 6, no bidentate carboxylate binding was observed; however, at both CN = 7 and 8, 35% of the carboxylate groups bound Ca^{2+} in a bidentate manner. Zn^{2+} behaved similarly in that, at CN = 4, only monodentate carboxylate ligands were found, but (as for Mn^{2+} and Ca^{2+}) bidentate carboxylate complexes were found at higher CNs (in 10% of structures with CN = 5 and 6 for Zn^{2+}). Among these cations, however, only Ca^{2+} shows a substantial number of bidentate carboxylate group ligands.

II. Energetic and Electron Distributions. a. Ligand Functionality in Divalent Manganese Complexes. The electronic

(29) Katz, A. K.; Glusker, J. P.; Beebe, S. A.; Bock, C. W. *J. Am. Chem. Soc.* **1996**, *118*, 5752−5763.

Table 2. Occurrences of $M^{2+}-O$, $M^{2+}-N$, $M^{2+}-S$, $M^{2+}-Cl$, and $M^{2+}-Br$ (M = Mg and Mn) Bonds Found in CSD[a]

	$Mg^{2+}-O$, $Mn^{2+}-O$		$Mg^{2+}-N$, $Mn^{2+}-N$		$Mg^{2+}-S$, $Mn^{2+}-S$		$Mg^{2+}-Cl$, $Mn^{2+}-Cl$		$Mg^{2+}-Br$, $Mn^{2+}-Br$		total no. of bonds	
CN	no.[b]	%	no.[b]	%	no.[b]	%	no.[b]	%	no.[b]	%	no.[b]	%
3	3	20.0	8	53.3	3	20.0	0	0.0	1	6.7	15	0.94
	9	25.0	18	50.0	6	16.7	3	8.3	0	0.0	36	1.1
4	47	35.6	60	45.4	3	2.3	13	9.8	9	6.8	132	8.2
	45	22.0	42	19.0	56	24.1	65	28.0	16	6.9	224	7.0
5	40	34.8	64	55.6	3	2.6	2	1.7	6	5.2	115	7.2
	77	32.8	104	44.2	20	8.5	25	10.6	9	3.8	235	7.3
6	934	77.1	196	16.2	0	0.0	65	5.4	17	1.4	1212	76.4
	1471	61.3	715	29.8	29	1.2	176	7.3	9	0.37	2400	75.0
7	81	72.3	22	19.6	0	0.0	9	8.0	0	0.0	112	7.0
	122	54.2	99	41.6	1	0.42	9	3.8	0	0.0	231	7.2
8	0	0.0	0	0.0	0	0.0	0	0.0	0	0.0	0	0.0
	44	61.1	28	38.9	0	0.0	0	0.0	0	0.0	72	2.2
$Mg^{2+}\cdots X$ for all ligands	1105	69.7	350	22.1	9	0.57	89	5.6	33	2.1	1586[c]	
$Mn^{2+}\cdots X$ for all ligands	1768	55.3	1006	31.4	112	3.5	278	8.7	34	1.2	3198[c]	

[a] Data for organic crystal structures, extracted from the CSD. Remeasurements of the same structure are not included in the count. For each coordination number, the upper entry is for Mg^{2+}, the lower entry for Mn^{2+}. [b] Number of $Mg^{2+}\cdots X$ and $Mn^{2+}\cdots X$ bonds. Percentages are also given for each individual coordination number.

Table 3. Metal Ion Coordination in Crystal Structures Containing $Mn^{2+}\cdots X$ (X = O, N, S, Cl, Br) in the CSD[a] (Number of Entries for Each Is Listed in Parentheses)

Coordination Number 3 (5 Entries)				
3N(2)	3S(1)			
2O1Br(1)	2N1O(1)			
Coordination Number 4 (33 Entries)				
4O(9)	4N(9)	4Br(1)	4Cl(2)	
3O1Br(1)	3N1O(3)	3N1S(1)	3N1Cl(1)	
2O2N(1)	2O2Br(1)	2N2S(1)	2N2Br(1)	2N2Cl(1)
Coordination Number 5 (23 Entries)				
5O(4)	5N(1)			
4N1O(11)	4N1Cl(1)	4Br1O(1)		
3O2N(1)	3N2O(1)	3S2N(1)		
2O2N1Cl(1)	2N2Br1O(1)			
Coordination Number 6 (202 Entries)				
6O(125)	6N(20)			
5O1N(7)	5O1Cl(2)			
4O2N(10)	4O2Br(3)	4O2Cl(5)	4N2O(8)	4N2Cl(1)
4Br2O(2)	4Cl2O(4)	4Cl2N(2)		
3O3N(3)	3O3Br(1)	3O3Cl(9)		
Coordination Number 7 (16 Entries)				
6O1Cl(2)				
5O2N(9)	5O1N1Cl(1)	5O2Cl(3)		
4O3N(1)				

[a] Listed are the ligand atoms around one manganese ion and, in parentheses, the number of individual crystal structures in which these are found. Individual refcodes of the CSD entries and their journal references are given in Table 1S (Supporting Information).

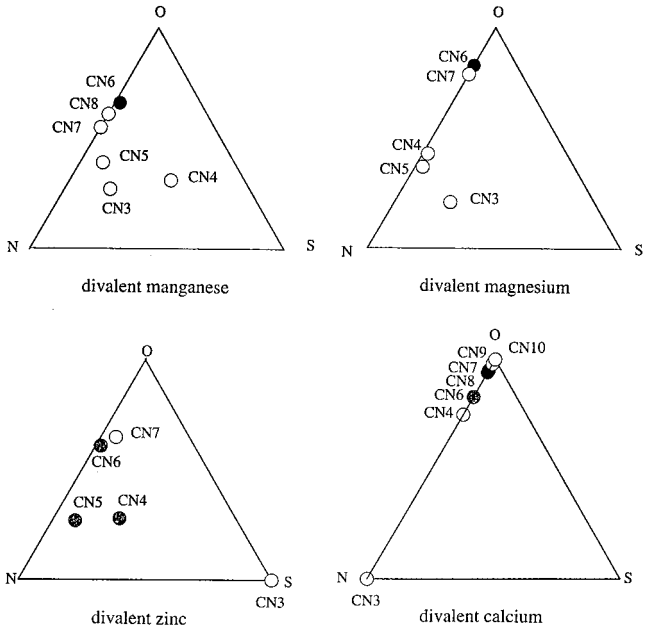

Figure 2. Binding plots, as triangular graphs, for O, N, S for various coordination numbers of divalent (a) manganese, (b) magnesium, (c) zinc, and (d) calcium. Data for these plots are derived from the CSD. 100% of one ligand atom (O, N, or S) is found at an apex of the triangle, as marked; percentages increase up the normal to the base of the equilateral triangle. Common coordination numbers are indicated by filled circles, fairly common ones by speckled circles, rare ones by open circles. If a metal ion binds *A*% to O, *B*% to N, and *C*% to S (where $A + B + C = 100$), the orthogonal coordinates are $X = [A/\tan 60°] + [C/\sin 60°]$, $Y = A$. Note that manganese shows a slightly higher preference than magnesium for nitrogen at high coordination numbers and a higher preference for sulfur at lower coordination numbers.

consequences of adding various ligands to Mn^{2+} were evaluated. To analyze the relative binding of O, N, and S to Mn^{2+} and Mg^{2+}, we initially optimized the complexes $M[NH_3]^{2+}$ and $M[H_2S]^{2+}$ (M = Mn or Mg) at the MP2(FULL)/6-311++G** computational level for comparison with the published results for $M[H_2O]^{2+}$.[30] Table 4 lists the calculated charges and natural electronic configuration for a variety of magnesium and manganese complexes; similar results for all the complexes in this paper can be found in Table 3S of the Supporting Information. It is evident from this table that more (negative) charge is transferred to the metal ion on going from O to N to S, and this effect is greater for Mn^{2+} (0.06e for O, 0.14e for N, 0.27e for S) than for Mg^{2+} (0.03e for O, 0.09e for N, 0.10e for S). Most of the additional electron density goes into the 3s and 4s orbitals for magnesium and manganese, respectively (see Table 4). The $M[H_2O]^{2+}$ complex is planar for both Mg and Mn, indicative of a very strong metal ion−dipole interaction, whereas the $M[SH_2]^{2+}$ complex is nonplanar for both metal ions, with a tilt angle of about 76.2° in each case (see Figure 3). This reflects the smaller dipole moment of H_2S compared to that of H_2O.

A comparison of M−O distances, binding enthalpies, and charges for the monohydrates $M[H_2O]^{2+}$ of the metal ions M in the neighborhood of manganese in the Periodic Table (Ca to Zn) is given in Table 4S of the Supporting Information, with values for Mg^{2+} for comparison.[30] These complexes are

(30) Trachtman, M.; Markham, G. D.; Glusker, J. P.; George, P.; Bock, C. W. *Inorg. Chem.* **1998**, *37*, 4421−4431.

Table 4. NPA Charges and Natural Electron Configurations for Selected Manganese and Magnesium Complexes

structure		metal	NPA charge on metal ion	NPA charge on liganding atoms	natural electron configuration of the metal ion
$M[H_2O]^{2+}$	**1**	Mg	+1.968	O, −1.104	Mg, [core]3s[0.02]3p[0.02][a]
		Mg	+1.968	O, −1.104	Mg, [core]3s[0.02]3p[0.02][c]
		Mn	+1.937	O, −1.083	Mn, [core]4s[0.03]3d[5.00]4p[0.02]4d[0.03]4f[0.02][a]
		Mn	+1.937	O, −1.066	Mn, [core]4s[0.04]3d[5.00]4p[0.02]4d[0.03]4f[0.02][d]
		Zn	+1.919	O, −1.093	Zn, [core]4s[0.08]3d[9.89]4p[0.03]4d[0.08]5p[0.01]4f[0.02][a]
$M[NH_3]^{2+}$	**2**	Mg	+1.910	N, −1.250	Mg, [core]3s[0.08]3p[0.02][a]
		Mn	+1.862	N, −1.214	Mn, [core]4s[0.11]3d[5.00]4p[0.02]4d[0.03]4f[0.02][a]
$M[H_2S]^{2+}$	**3**	Mg	+1.898	S, −0.467	Mg, [core]3s[0.07]3p[0.01]3d[0.01]4p[0.01][a]
(nonplanar)		Mn	+1.726	S, −0.171	Mn, [core]4s[0.20]3d[5.01]4p[0.04]4d[0.03]5p[0.01]4f[0.02][a]
$M[H_2O]_6^{2+}$	**4**	Mg	+1.799	O, −1.005	Mg, [core]3s[0.17]3p[0.02]3d[0.01]4p[0.01][b]
		Mn	+1.703	O, −1.040	Mn, [core]4s[0.22]3d[5.05]4p[0.02]4d[0.02][f]
		Mn	+1.687	O, −0.976	Mn, [core]4s[0.16]3d[5.08]4p[0.02]4d[0.05]5p[0.01]4f[0.02]5d[0.02][d]
		Zn	+1.743	O, −0.988	Zn, [core]4s[0.22]3d[9.89]4p[0.03]5s[0.01]4d[0.08]5p[0.01]4f[0.02] 5*d*[0.02][d]
$M[H_2O]_4^{2+}\cdot[NH_3]_2$	**7**	Mg	+1.759	O, −0.986	Mg, [core]3s[0.21]3p[0.02]3d[0.01]4p[0.01][c]
				N, −1.119	
		Mn	+1.657	O, −1.020	Mn, [core]4d[0.27]3d[5.04]4p[0.03]4d[0.02][e]
				N, −1.213	
		Mn	+1.636	O, −0.968	Mn, [core]4s[0.21]3d[5.08]4p[0.02]4d[0.05]5p[0.01]4f[0.02]5d[0.02][d]
				N, −1.099	
		Zn[j]	+1.671	O, −0.977	Zn, [core]4s[0.29]3d[9.89]4p[0.04]5s[0.01]4d[0.08]5p[0.01]4f[0.02] 5*d*[0.02][d]
				N, −1.108	
$M[NH_3]_6^{2+}$	**8**	Mg	+1.702	N, −1.106	Mg, [core]3s[0.26]3p[0.02]3d[0.01]4p[0.01][c]
		Mn	+1.581	N, −1.196	Mn, [core]4s[0.34]3d[5.05]4p[0.03]4d[0.02][e]
		Mn	+1.547	N, −1.086	Mn, [core]4s[0.27]3d[5.09]4p[0.03]4d[0.05]5p[0.01]4f[0.02]5d[0.03][d]
$M[H_2O]_5^{2+}\cdot[OH^-]$	9	Mg	+1.786	O, −1.366[h]	Mg, [core]3s[0.18]3p[0.02]3d[0.02]4p[0.01][b]
				O, −0.976 → −1.020[g]	
		Mn	+1.649	O, −1.279[h]	Mn, [core]4s[0.24]3d[5.06]4p[0.04]4d[0.02][e]
				O, −1.002 → −1.034[g]	
		Mn	+1.633	O, −1.290[h]	Mn, [core]4s[0.17]3d[5.11]4p[0.02]4d[0.05]5p[0.01]4f[0.02]5d[0.02][d]
				O, −0.952 → −0.989[g]	
$M[H_2O]_5^{2+}\cdot[HCO_2^-]$	**11**	Mg	+1.765	O, −0.977 → −1.015[g]	Mg, [core]3s[0.19]3p[0.02]3d[0.02]4p[0.01][b]
(two hydrogen bonds)		Mn	+1.654	O, −1.007 → −1.030[g]	Mn, [core]4s[0.25]3d[5.05]4p[0.04]4d[0.02][e]
		Mn	+1.618	O, −0.949 → −0.976[g]	Mn, [core]4s[0.19]3d[5.10]4p[0.02]4d[0.06]5p[0.01]4f[0.02]5d[0.02][d]

[a] MP2(FULL)/6-311++G**//MP2(FULL)/6-311++G** computational level; MP2 density. [b] MP2(FULL)/6-311++G**//MP2(FC)/6-31+G* computational level; MP2 density. [c] MP2(FULL)/6-311++G**//HF/6-31G* computational level; MP2 density. [d] MP2(FULL)/6-311++G**//HF/HUZ* computational level; MP2 density. [e] MP2(FULL)/HUZ*//HF/HUZ* computational level; MP2 density. [f] MP2(FULL)/HUZ*//MP2(FULL)/HUZ* computational level; MP2 density. [g] Water oxygen atoms. [h] Hydroxyl oxygen atom.

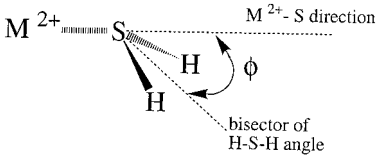

Figure 3. Tilt angle ϕ for $M[H_2S]^{2+}$ (where M = Mg, Mn).

sufficiently small to allow high-level MP2(FULL)/6-311++G** optimizations to be performed in all cases, followed by single-point CCSDT(FULL)/6-311++G** calculations to obtain reliable energies. Several of the M−O distances (e.g., those involving Cr^{2+} and Fe^{2+}) are similar to the Mg−O distance of 1.957 Å in $Mg[H_2O]^{2+}$. The binding energy of the monohydrate $Mg[H_2O]^{2+}$ is closest to that of $Mn[H_2O]^{2+}$, and the calculated NPA charges on the metal ions in these monohydrates are closer for magnesium and manganese than they are for magnesium and most of the other transition metal elements.[30] The enthalpy change for the decomposition of $Ca[H_2O]^{2+}$ (54.6 kcal/mol) is significantly smaller than that for the first-row transition metal ions (66.5−102.5 kcal/mol).[30] The Zn−O distance in the monohydrate $Zn[H_2O]^{2+}$ is found to be shorter than the metal−oxygen distances in the corresponding Mg^{2+} and Mn^{2+} monohydrates by 0.08 and 0.12 Å, respectively.

Of the various manganese complexes, those with a coordination number of 6 are the most relevant to systems of biological interest. The structures of a wide variety of six-coordinate hydrates, ammoniates, hydroxylates, and carboxylates of divalent manganese have also been studied by ab initio molecular orbital calculations, and the formulas are shown in Figure 4. Detailed structures, with geometries and charge distributions, are shown in Figure 1S and atomic coordinates in Table 5S of the Supporting Information. Total molecular energies, thermal corrections, and entropies of all the structures in Figure 4 are given in Table 6S of the Supporting Information. The ground state of each of these divalent manganese complexes is, as expected, a sextuplet with one electron in each of the five d-orbitals. The analogous structural and energetic data for the corresponding magnesium complexes with singlet ground states are given in the Supporting Information to the paper by Katz et al.[11]

Since most optimizations on the larger manganese complexes could only be performed at the HF/HUZ* level, it is important to establish how well this method performs in comparison to more sophisticated computational methods. In Table 5, we compare the Mn−O distances and the NPA charge on the manganese ion in the $Mn[H_2O]^{2+}$ and $Mn[H_2O]_6^{2+}$ complexes at several computational levels. It is evident from this table that the HF/HUZ* and HF/6-311++G** levels yield similar Mn−O distances and NPA charges on the Mn^{2+} ion. The MP2(FULL)/HUZ*, MP2(FULL)/6-311++G**, and B3LYP/6-311++G** levels, which include the effects of electron correlation, give Mn−O distances which are smaller than those found with the HF methods; e.g., correlation effects reduce the Mn−O distance in $Mn[H_2O]_6^{2+}$ by 0.02−0.03 Å. These smaller Mn−O distances are accompanied by a greater transfer of electronic charge from

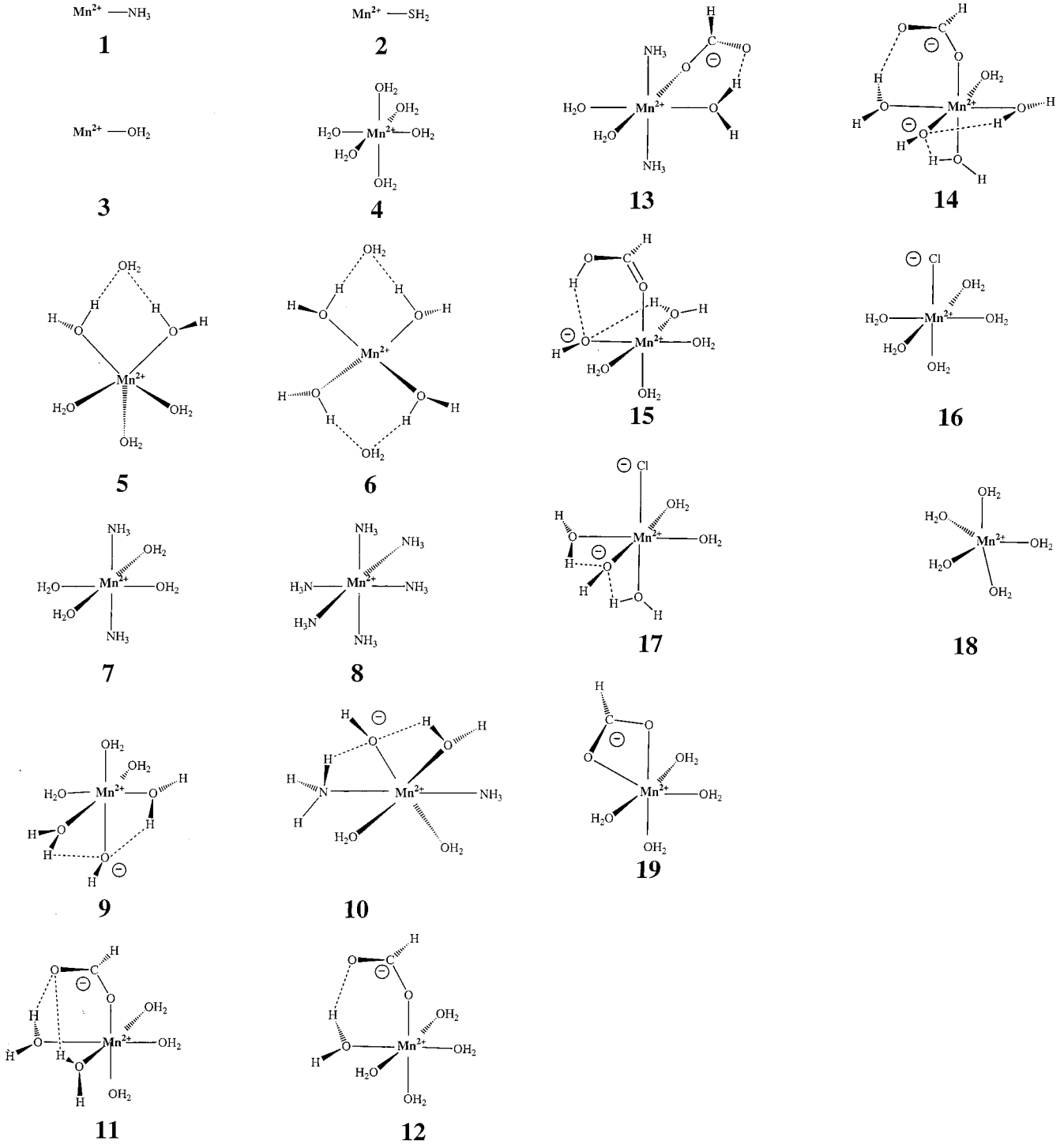

Figure 4. Schematic diagrams of $Mn[NH_3]^{2+}$ (**1**), $Mn[SH_2]^{2+}$ (**2**), $Mn[H_2O]^{2+}$ (**3**), $Mn[H_2O]_6^{2+}$ (**4**), $Mn[H_2O]_5^{2+}\cdot H_2O$ (**5**), $Mn[H_2O]_4^{2+}\cdot 2H_2O$ (**6**), $Mn[H_2O]_4^{2+}\cdot[NH_3]_2$ (**7**), $Mn[NH_3]_6^{2+}$ (**8**), $Mn[H_2O]_5^{2+}\cdot[OH^-]$ (**9**), $Mn[H_2O]_3^{2+}\cdot[NH_3]_2\cdot[OH^-]$ (**10**), $Mn[H_2O]_5^{2+}\cdot[HCO_2^-]$ (two hydrogen bonds) (**11**), $Mn[H_2O]_5^{2+}\cdot[HCO_2^-]$ (one hydrogen bond) (**12**), $Mn[H_2O]_3^{2+}\cdot[NH_3]_2\cdot[HCO_2^-]$ (**13**), $Mn[H_2O]_4^{2+}\cdot[HCO_2^-]\cdot[OH^-]$ (**14**), $Mn[H_2O]_4^{2+}\cdot[HCO_2H]\cdot[OH^-]$ (**15**), $Mn[H_2O]_5^{2+}\cdot[Cl^-]$ (**16**), $Mn[H_2O]_4^{2+}\cdot[Cl^-]\cdot[OH^-]$ (**17**), $Mn[H_2O]_5^{2+}$ (**18**), and $Mn[H_2O]_4^{2+}\cdot[HCO_2^-]$ (bidentate) (**19**).

the water ligands to the Mn^{2+} ion. It should be noted, however, that such relatively small changes in the geometry of these complexes do not significantly alter calculated binding energies obtained from subsequent single-point calculations.[31]

The octahedral (T_h) manganese complex $Mn[H_2O]_6^{2+}$ (**4**) is a local minimum on the potential energy surface, as are similar complexes for $M[H_2O]_6^{2+}$ (M = Mg or Zn) (as well as Ca-$[H_2O]_6^{2+}$, although Ca^{2+} complexes often have coordination numbers greater than 6).[13,14,29,31,32] It should be noted that there is evidence from blackbody infrared radiative dissociation (BIRD) experiments of a second conformer of the hexahydrated Mg^{2+} ion in the gas phase at higher temperatures (~80 °C);[33,34] hexahydrated Ca^{2+} apparently does not have a second con-

(31) Pavlov, M.; Siegbahn, P. E. M.; Sandström, M. *J. Phys. Chem.* **1998**, *A102*, 219−228.

(32) Tongraar, A.; Liedl, K. R.; Rode, B. M. *J. Phys. Chem. A* **1997**, *101*, 6299−6309.

(33) Rodriguez-Cruz, S. E.; Jockusch, R. A.; Williams, E. R. *J. Am. Chem. Soc.* **1999**, *121*, 1986−1987.

Table 5. Comparison of Calculated Mn−O Distances and NPA Charge[9] on the Manganese Ions in $Mn[H_2O]^{2+}$ and $Mn[H_2O]_6^{2+}$ at a Variety of Computational Levels

	$Mn[H_2O]^{2+}$		$Mn[H_2O]_6^{2+}$	
level	Mn−O (Å)	q_{Mn}	Mn−O (Å)	q_{Mn}
HF/HUZ*//HF/HUZ*	2.050	1.956	2.246	+1.795
MP2(FULL)/HUZ*// MP2(FULL)/HUZ*	2.018	1.929	2.221	+1.703
HF/6-311++G**// HF/6-311++G**	2.047	1.962	2.254	+1.795
MP2(FULL)/6-311++G**// MP2(FULL)/6-311++G**	2.007	1.933		
B3LYP/6-311++G**// B3LYP/6-311++G**	1.988	1.886	2.218	+1.612

former, and no data are currently available for hexahydrated Mn^{2+}. The calculated structure of the $Mn[H_2O]_6^{2+}$ complex appears to be similar to that observed in frozen aqueous solutions of $MnCl_2$ using distance-dependent enhanced ^1H electron−nuclear double-resonance spectroscopy. In this experiment, the Mn^{2+}−H distance was found to be 2.90 Å,[35,36] indicating that hydration of Mn^{2+} had occurred; the calculated Mn^{2+}−H distance for $Mn[H_2O]_6^{2+}$ is 2.918 Å at the HF/HUZ* computational level.

The metal−oxygen bonding in $Mn[H_2O]_6^{2+}$ is predominantly electrostatic. More electron density (0.31e) is transferred to the manganese ion in $Mn[H_2O]_6^{2+}$ than to the magnesium ion in $Mg[H_2O]_6^{2+}$ (0.20e), although the calculated Mn−O distances of 2.246 Å are approximately 0.1 Å greater than the Mg−O distances; the result for $Zn[H_2O]_6^{2+}$ (0.26e) is between those for magnesium and manganese. The charges on the water oxygen atoms in $Mn[H_2O]_6^{2+}$ (−0.98e) are slightly more negative than those in isolated water (−0.90e) but less negative than those in $Mg[H_2O]_6^{2+}$ (−1.01e) or $Zn[H_2O]_6^{2+}$ (−0.99e). A significant portion of the charge density transferred to the central ion resides in the 3s orbital for Mg^{2+} and the 4s orbitals for Mn^{2+} and Zn^{2+}. Mn^{2+} also gains some electron density in the 3d orbitals, whereas Zn^{2+} loses electron density in these orbitals.

To provide a more rigorous basis for comparison of the structures of hexahydrated Mg^{2+}, Mn^{2+}, and Zn^{2+} complexes, we optimized $M[H_2O]_6^{2+}$ (M = Mg, Mn, and Zn) using density functional theory at the B3LYP/6-311++G** level. This method incorporates the effects of electron correlation into the calculated geometrical parameters. The results of the optimizations are given in Table 6,[37−41] together with the NPA atomic charges; for comparison, we also list in this table the metal−oxygen distances in some citrate crystal structures. Hartmann and co-workers[14] have recently reported the results of optimizations on $Zn[H_2O]_6^{2+}$ (as well as for several other hydrated divalent zinc complexes) using density functional theory with similar basis sets. Our calculated Zn−O distances are in excellent agreement with their results. For these complexes, the Mn−O distance is (as found earlier in the CSD search) approximately 0.1 Å greater than the Mg−O distance, while the Zn−O distance is only 0.016 Å greater than that involving Mg^{2+}. Furthermore, the calculated charge distribution in $Mg[H_2O]_6^{2+}$ is closer to that in $Zn[H_2O]_6^{2+}$ than to that in $Mn[H_2O]_6^{2+}$. Thus, it might appear that Zn^{2+} would be a better replacement for Mg^{2+} in biological systems than would Mn^{2+}. Since this is generally not the case experimentally, other factors must also be important and intervene.

Coordination requirements of the metal ions were then considered. Optimizations of $Mn[H_2O]_5^{2+}\cdot H_2O$ (**5**) and $Mn[H_2O]_4^{2+}\cdot 2H_2O$ (**6**), with one and two water molecules, respectively, in the second hydration sphere surrounding Mn^{2+}, were also carried out at the HF/HUZ* computational level. Energies of these complexes are higher than those of $Mn[H_2O]_6^{2+}$ (see Table 7); values for the corresponding magnesium complexes are also given in this table. Within the context of a hexahydrated complex, there is clearly a greater energy penalty for changing the inner-shell coordination number of Mg(II) than of Mn(II), suggesting somewhat less rigid coordination requirements for manganese complexes. Similar calculations were done for $Zn[H_2O]_6^{2+}$, $Zn[H_2O]_5^{2+}\cdot H_2O$, and $Zn[H_2O]_4^{2+}\cdot 2H_2O$. For Mn(II) complexes, the energetics of CN change are between those for Zn^{2+} and Mg^{2+} (Table 7).[10,13] At some computational levels, $Zn[H_2O]_4^{2+}\cdot 2H_2O$ is found to be slightly lower in energy than $Zn[H_2O]_6^{2+}$.[31] The coordination requirements for divalent zinc are apparently significantly less rigid than those for divalent magnesium or manganese. This is in line with the work of others. Relativistic pseudopotential calculations by Sponer and co-workers[42] on the interaction between several pentahydrated metal ions, such as Mg^{2+} and Zn^{2+}, and the guanine-cytosine Watson−Crick DNA base pair show that Zn^{2+} is more tightly bound to the bases (presumably mainly via N) than is Mg^{2+}, while the hydration shell around Zn^{2+} is more flexible than that of Mg^{2+}.

The search of crystal structures in the CSD showed a greater preference for nitrogen ligands by manganese than by magnesium. To analyze the energetic implications of the observation, we optimized one conformer of $Mn[H_2O]_4^{2+}\cdot[NH_3]_2$ and also $Mn[NH_3]_6^{2+}$ (see structures **7** and **8** in Figure 4). The presence of the two NH_3 ligands in **7** leads to an increase in the four Mn−O distances by nearly 0.05 Å compared to those in $Mn[H_2O]_6^{2+}$. In $Mn[NH_3]_6^{2+}$, the Mn−N distances are about 0.12 Å longer than the Mg−N distances in $Mg[NH_3]_6^{2+}$. More charge is transferred to the metal ions in $M[H_2O]_4^{2+}\cdot[NH_3]_2$ and $M[NH_3]_6^{2+}$ than in $M[H_2O]_6^{2+}$ for both magnesium and manganese (to the 3s and 4s orbitals, respectively), but the bonding remains primarily electrostatic (see Table 4).

Reactions in which nitrogen-containing ligands are transferred from magnesium to manganese ions, i.e.,

$$Mn[H_2O]^{2+} + Mg[NH_3]^{2+} \rightarrow Mn[NH_3]^{2+} + Mg[H_2O]^{2+}$$

$$Mn[H_2O]_6^{2+} + Mg[H_2O]_4^{2+}\cdot[NH_3]_2 \rightarrow Mn[H_2O]_4^{2+}\cdot[NH_3]_2 + Mg[H_2O]_6^{2+}$$

and

$$Mn[H_2O]_6^{2+} + Mg[NH_3]_6^{2+} \rightarrow Mn[NH_3]_6^{2+} + Mg[H_2O]_6^{2+}$$

are all exothermic (see Table 8a). This confirms that manganese is more accepting of liganding nitrogen atoms than is magne-

(34) Rodriguez-Cruz, S. E.; Jockusch, R. A.; Williams, E. R. Personal communication.

(35) Sivaraja, M.; Stouch, T. R.; Dismukes, G. C. *J. Am. Chem. Soc.* **1992**, *114*, 9600−9603.

(36) Zheng, M.; Dismukes, G. C. *J. Phys. Chem. B* **1998**, *102*, 8306−8313.

(37) Johnson, C. K. *Acta Crystallogr.* **1965**, *18*, 1004−1018.

(38) Carrell, H. L.; Glusker, J. P. *Acta Crystallogr.* **1973**, *B29*, 638−640.

(39) Swanson, R.; Ilsley, W. H.; Stanislowski, A. G. *J. Inorg. Biochem.* **1983**, *18*, 187−194.

(40) Tsuji, S.; Shibata, T.; Ito, Y.; Fujii, S.; Tomita, K.-I. *Acta Crystallogr.* **1991**, *C47*, 528−531.

(41) Sheldrick, B. *Acta Crystallogr.* **1974**, *B30*, 2056−2057.

(42) Sponer, J.; Burda, J. V.; Sabat, M.; Leszczynski, J.; Hobza, P. *J. Phys. Chem. A* **1998**, *102*, 5951−5957.

Table 6. Comparison of Geometrical Parameters and Charge Distribution of the Hexahydrates $M[H_2O]_6^{2+}$ (M = Mg, Mn, Zn, and Ca) at the B3LYP/6-311++G**//B3LYP/6-311++G** Computational Level (Distances in Å, Angles in Deg, Charges in Electrons)

			geometrical parameters[b]			NPA charges[c]		
M^{2+}	distance in citrates[a]	ref	M−O	O−H	∠MOH	M	O	H
Mg	2.07(0.001)	37	2.113	0.967	126.7	+1.819	−1.016	+0.523
Mn	2.17(0.002)	38	2.218	0.968	126.7	+1.612	−0.983	+0.524
Zn	2.09(0.003)	39, 40	2.129	0.967	126.2	+1.740	−1.006	+0.524
Ca[d]	2.42(0.005)	41	2.414	0.974	127.4	+1.898	−1.064	+0.540

[a] From X-ray structures in the CSD. Estimated standard deviations are given in parentheses (from the published crystal structures). [b] From density functional calculations at the B3LYP/6-311++G**//B3LYP/6-311++G** level. [c] Natural electron configuration: Mg, $3s^{0.17}3p^{0.01}$; Mn, $4s^{0.16}3d^{5.20}4d^{0.02}$; Zn, $4s^{0.24}3d^{9.99}4p^{0.01}4d^{0.01}$; Ca, $4s^{0.09}3d^{0.01}$. [d] Huzinaga basis set including diffuse functions; see ref 29.

Table 7. Relative Energies, ΔE (kcal/mol), of $M[H_2O]_6^{2+}$, $M[H_2O]_5^{2+}\cdot H_2O$, and $M[H_2O]_4^{2+}\cdot 2H_2O$ (M = Mg, Mn, Zn)

	relative energies, ΔE,[c] MP2(FULL)/6-311++G**//HF[a] level		
	Mg[e]	Mn	Zn[f]
$M[H_2O]_6^{2+}$	0.0	0.0	0.0
$M[H_2O]_5^{2+}\cdot H_2O$[d]	+6.4	+3.5	+1.0
	(+6.8)[b]	(+4.1)[b]	(+1.6)[b]
$M[H_2O]_4^{2+}\cdot 2H_2O$[d]	+12.4	+7.7	+1.4
	(+13.2)[b]	(+8.9)[b]	(+1.9)[b]

[a] HF = HF/6-31G* for magnesium compounds and HF/HUZ* for manganese and zinc compounds. [b] Values in parentheses have been adjusted to 298 K using the HF vibrational frequency analyses. [c] $\Delta E = E\{M[H_2O]_6^{2+}\} - E\{M[H_2O]_n^{2+}\cdot mH_2O\}$, $n = 6, 5, 4$; $m = 0, 1, 2$; $n + m = 6$; M = Mg, Mn, Zn. Note that, when $n = 6$ and $m = 0$, $\Delta E = 0.0$, as shown in the first line of the table. Positive values indicate the weakness of a complex relative to $M[H_2O]_6^{2+}$. [d] The second-shell water molecules are hydrogen bonded to two first-shell water molecules (see Figure 4). [e] Pavlov et al.[31] find the same ordering at the B3LYP/6-311+G(2d,2p)//B3LYP/LANL2DZ level, but the energy differences are smaller, +3.7 kcal/mol for $Mg[H_2O]_5^{2+}\cdot H_2O$ and +4.4 kcal/mol for $Mg[H_2O]_4^{2+}\cdot 2H_2O$. [f] Pavlov et al.[31] find that $Zn[H_2O]_4^{2+}\cdot 2H_2O$ is lowest in energy at the B3LYP/6-311+G(2*d*,2*p*)//B3LYP/LANL2DZ level. $Zn[H_2O]_6^{2+}$ is +3.4 kcal/mol, and $Zn[H_2O]_5^{2+}\cdot H_2O$ is +3.7 kcal/mol.

sium. The value of ΔH°_{298} for the transfer reaction $Mg^{2+} + Mn[H_2O]_6^2 \rightarrow Mg[H_2O]_6^{2+} + Mn^{2+}$ is significantly exothermic (see Table 9), confirming an energetic preference of magnesium for water, as was implied by the results of the CSD search (see Figure 2). Interestingly, the corresponding transfer reaction between magnesium and zinc (Table 9) is substantially endothermic. The crystal structures present in the CSD in which different pairs of metal ions were present (e.g., Mg and Mn, or Mn and Zn, etc.) indicate that the ions exhibit the anticipated ligand preferences in the condensed phases (see Table 8b).[43−50] This table leads to the conclusion that Mg^{2+} and Ca^{2+} bind oxygen atoms in ligands if they are available, while Zn^{2+} will accept oxygen or nitrogen or sulfur for binding. Mn^{2+} binds nitrogen but has a preference for oxygen. In this it is different from Zn^{2+}.

b. Energetics of Ionization and Proton Transfer in Mn(II)-Bound Water. The ionization of water is facilitated by metal ions, and this property can be utilized by enzymes to generate hydroxyl or hydrogen ions for catalysis. Removal of a hydrogen ion from one water molecule in $Mn[H_2O]_6^{2+}$ and in $Mn[H_2O]_4^{2+}\cdot[NH_3]_2$, with subsequent reoptimization, yields structures **9** and **10**, respectively (see Figure 4). Two of the water molecules in $Mn[H_2O]_5^{2+}\cdot[OH^-]$ are directly involved in hydrogen-bonding interactions with the hydroxyl group, although the O···H distances (1.956 and 2.026 Å) are not the same. We observed a similar situation for the corresponding

Table 8. Competition between Metal Ions for Various Ligands

(a) Enthalpy Changes, ΔH°_{298} (kcal/mol), and Free Energy Changes, ΔG°_{298} (kcal/mol), for Various Transfer Reactions of Mg^{2+} and Zn^{2+}, Showing Ligand Selection among Water and Ammonia (O versus N)

reaction	ΔH°_{298}	ΔG°_{298}
$Mn[H_2O]^{2+} + Mg[NH_3]^{2+} \rightarrow Mn[NH_3]^{2+} + Mg[H_2O]^{2+}$	−2.9[a]	−2.8[a]
$Mn[H_2O]_6^{2+} + Mg[H_2O]_4^{2+}\cdot[NH_3]_2 \rightarrow Mn[H_2O]_4^{2+}\cdot[NH_3]_2 + Mg[H_2O]_6^{2+}$	−5.1[b]	-4.3[b]
$Mn[H_2O]_6^{2+} + Mg[NH_3]_6^{2+} \rightarrow Mn[NH_3]_6^{2+} + Mg[H_2O]_6^{2+}$	−10.8[b]	−10.3[b]

(b) Competition for O, N, S, Cl in Crystal Structures in the CSD That Contain Two Different Metal Ions from among Mn^{2+}, Mg^{2+}, Zn^{2+}, and Ca^{2+}

	coordination					
metal ions	Mn^{2+}	Mg^{2+}	Zn^{2+}	Ca^{2+}	CSD refcode	ref
Zn, Ca			N, 3O	6O	GAWMOG	43
Mg, Zn		6O	4O, N		GAWMIA	43
		6O	4O, 2N		ZNEDTA12	44
		6O	4O, N		KIKRIF	45
Mn, Zn	6O		N, 3O		GAWLIZ	43
	6O		4O		ZAQSIT	46
	6O		5O		POMWUJ10	47a,b
	6O		4Cl		HEBMEG	48
	4N, 2S		4S		RUDRUD	49
	3N, 3O		6N		VONNER	50

[a] MP2(FULL)/6-311++G**//MP2(FULL)/6-311++G** computational level. [b] MP2(FULL)/6-311++G**//HF/6-31G* for the magnesium complexes and MP2(FULL)/6-311++G**//HF/HUZ* for the manganese complexes.

Table 9. Metal Ion-Hydrated Metal Complex-Transfer Reactions

	ΔH°_{298} (kcal/mol)	
reaction	B3LYP/6-311++G**//B3LYP/6-311++G**[a]	MP2(FULL)/6-311G**//HF[a]
$Mg^{2+} + Mn[H_2O]_6^{2+} \rightarrow Mg[H_2O]_6^{2+} + Mn^{2+}$	−13.4	−19.4
$Mg^{2+} + Zn[H_2O]_6^{2+} \rightarrow Mg[H_2O]_6^{2+} + Zn^{2+}$	+25.9	+19.2

[a] Frequency analyses at the HF level were used for thermal corrections giving ΔH°_{298}.

(43) Clegg, W.; Little, I. R.; Straughan, B. P. *Inorg. Chem.* **1988**, *27*, 1916−1923.
(44) Solans, X.; Font-Altaba, M.; Oliva, J.; Herrera, J. *Acta Crystallogr. C* **1983**, *39*, 435−438.
(45) Clegg, W.; Harbron, D. R.; Straughan, B. P. *Acta Crystallogr.* **1991**, *47*, 267−270.
(46) Drumel, S.; Bujoli-Doeuff, M.; Janvier, P.; Bujoli, B. *New J. Chem.* (*Nouv. J. Chim.*) **1995**, *19*, 239−242.
(47) (a) Tanase, T.; Watton, S. P.; Lippard, S. J. *J. Am. Chem. Soc.* **1994**, *116*, 9401−9402. (b) Tanase, T.; Yun, J. W.; Lippard, S. J. *Inorg. Chem.* **1996**, *35*, 3585−3594.
(48) Furmanova, N. G.; Kozhoeva, S. T.; Sulaimankulov, K.; Resnyanskii, V. F. *Kristallografiya* **1993**, *38*, 120−125.
(49) Mikuriya, M.; Tsutsumi, H.; Nukada, R.; Handa, H.; Sayama, Y. *Bull. Chem. Soc. Jpn.* **1996**, *69*, 3489−3498.
(50) Chaudhuri, P.; Winter, M.; Birkelbach, F.; Fleischhauer, P.; Haase, W.; Florke, U.; Haupt, H.-J. *Inorg. Chem.* **1991**, *30*, 4291−4293.

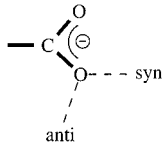

Figure 5. Syn and anti orientations of metal ion−carboxylate interactions.

magnesium complex.[11] In the particular structure of $Mn[H_2O]_3^{2+}\cdot[OH^-]\cdot[NH_3]_2$ that we optimized, only one water ligand is hydrogen bonded to the hydroxyl oxygen atom (1.833 Å), but there is also a long (weak) hydrogen bond involving a hydrogen atom from one of the NH_3 ligands (2.300 Å). The manganese−oxygen bonding remains primarily electrostatic in both $Mn[H_2O]_5^{2+}\cdot[OH^-]$ and $Mn[H_2O]_3^{2+}\cdot[OH^-]\cdot[NH_3]_2$, although some additional charge density is transferred into the 3d-orbitals on the manganese ion (see Table 3S, Supporting Information). Interestingly, the difference in NPA charge on the manganese ion between $Mn[H_2O]_6^{2+}$ (+1.687) and $Mn[H_2O]_5^{2+}\cdot[OH^-]$ (+1.633) is about 4 times greater than that between the corresponding magnesium complexes (+1.799 and +1.786, respectively), where the 3d-orbitals play no significant role in bonding. Bertini and co-workers[51] have shown that the Mulliken charges on the divalent zinc ions in $Zn[NH_3]_5^{2+}\cdot[H_2O]$ and $Zn[NH_3]_5^{2+}\cdot[OH^-]$, where the five d-orbitals are completely filled, are very similar to each other. In this, zinc therefore resembles our data on Mg^{2+} but not Mn^{2+} (presumably because divalent manganese has only partially filled d-orbitals).

To evaluate the structural and energetic consequences of replacing an inner-sphere water molecule with a carboxylate ligand, two local minima of $Mn[H_2O]_5^{2+}\cdot[HCO_2^-]$ on the potential energy surface were identified at the HF/HUZ* level (see structures **11** and **12** in Figure 4). In the lowest energy form, **11**, the carboxylate oxygen atom that is not bound to the manganese ion interacts with hydrogen atoms from two different inner-sphere water molecules. In the second form, **12**, only one such interaction is present, and this form is 1.4 kcal/mol higher in energy at the MP2(FULL)/6-311++G**//HF/HUZ* level. The manganese ions in these complexes are in a syn orientation relative to the carboxylate group (see Figure 5).[52] When the $Mn[H_2O]_5^{2+}\cdot[HCO_2^-]$ complex structure was initialized in an anti orientation, it isomerized to a syn form during the optimization; this was also observed with the corresponding magnesium complex.[11,53] It should be noted that, while the carboxylate−water interaction motif **12** is found in a variety of crystal structures in the current versions of the CSD and PDB,[10,11] no entries containing the motif in **11** are found. Binding enthalpies and free energies for the carboxylate group in $M[H_2O]_5^{2+}\cdot[HCO_2^-]$ (M = Mg, Mn, and Zn) are compared in Table 10a, where it can be seen that there is relatively little difference among the three metal ions. For comparison, we also optimized one conformer of $Mn[H_2O]_3^{2+}\cdot[HCO_2^-]\cdot[NH_3]_2$, which is shown as structure **13** in Figure 4. Because of the position of the two NH_3 groups, the carboxylate oxygen atom that is not bound to the manganese ion in this structure interacts with only one water hydrogen atom. The O−H···O distance is nearly 0.1 Å longer than that in the corresponding structure, **12**, suggesting a weaker hydrogen bond. Comparison of the experimental values for carboxylate dissociation in aqueous solution (Table 10b)[54] with the computed (gas phase) values shows the same relative order of affinity among Zn, Mg, and Mn. However, the quantitative differences among the cations are apparently attenuated in solution.

Table 10

(a) Enthalpy Changes, ΔH°_{298} (kcal/mol), and Free Energy Changes, ΔG°_{298} (kcal/mol), for the Reaction $M[H_2O]_5^{2+}\cdot[HCO_2^-] \rightarrow M[H_2O]_5^{2+} + HCO_2^-$) (M = Mg, Mn, and Zn)

	MP2(FULL)/6-311++G**//HF[a]	
metal	ΔH°_{298}	ΔG°_{298}
Mg	+229.1	215.9
Mn	+226.0	213.1
Zn	+229.8	217.0

(b) Relative Free Energy Change ($\Delta\Delta G$, kcal/mol) for Carboxylate Dissociation

	gas phase[b]	aqueous solution[c,54]
Zn	0	0
Mg	+1.1	+1.2
Mn	+3.9	+1.4

[a] HF/6-31G* for the magnesium complexes and HF/HUZ* for the manganese and zinc complexes. The thermal corrections and entropies for the calculation of ΔH°_{298} and ΔG°_{298} are given in Table 1S (Supporting Information) or in refs 10 and 11. [b] Computed values. [c] Experimental values.

Since extensive calculations on several conformers of the magnesium complexes $Mg[H_2O]_4^{2+}\cdot[OH^-]\cdot[HCO_2^-]$ showed little variation in energy,[11] we considered only a single conformer of $Mn[H_2O]_4^{2+}\cdot[OH^-]\cdot[HCO_2^-]$, which is illustrated schematically as structure **14** in Figure 4. The manganese ion is in a syn orientation relative to the carboxylate group in this conformer, and no attempt was made to find an anti structure. It should be noted that the carboxylate oxygen atom forms a hydrogen bond with only one water molecule, and that there are intramolecular interactions between two water molecules and the hydroxyl group.

The HF/HUZ*-optimized form of $Mn[H_2O]_4^{2+}\cdot[OH^-]\cdot[HCOOH]$ is shown as structure **15** in Figure 4. This complex has a relatively short O···H hydrogen bond (1.512 Å) between the hydroxyl oxygen atom and the acidic hydrogen atom in formic acid. The complex $Mn[H_2O]_4^{2+}\cdot[OH^-]\cdot[HCOOH]$ is approximately 4.4 kcal/mol *higher* in energy than conformer **12** of $Mn[H_2O]_5^{2+}\cdot[HCO_2^-]$ at the MP2(FULL)6-311++G**//HF/HUZ* computational level. Interestingly, an attempt to find a local minimum of $Mn[H_2O]_4^{2+}\cdot[OH^-]\cdot[HCOOH]$ at the B3LYP/HUZ* level, which incorporates electron correlation into the optimization, failed, and the optimization gave $Mn[H_2O]_5^{2+}\cdot[HCO_2^-]$. Similar results were found for optimizations of the magnesium complex $Mg[H_2O]_4^{2+}\cdot[OH^-]\cdot[HCOOH]$, where MP2(FC)/6-31+G* level calculations also failed to identify this structure as a local minimum on the corresponding potential energy surface.[11] On the other hand, calculations on $Mg[H_2O]_4^{2+}\cdot[OH^-]\cdot[RCOOH]$ showed that, when R is an electron-donating group such as $-NH_2$, this structure is a local minimum on the potential energy surface at the MP2(FC)/6-31+G* level.[11]

Two reactions of aquo manganese complexes were studied. In the first reaction, one water molecule in $Mn[H_2O]_6^{2+}$, $Mn[H_2O]_4^{2+}\cdot[NH_3]_2$, or $Mn[H_2O]_5^{2+}\cdot[HCO_2^-]$ ionizes; i.e., one of the deprotonation reactions occurs:

(51) Bertini, I.; Luchinat, C.; Rosi, M.; Sgamellotti, A.; Tarantelli, F. *Inorg. Chem.* **1990**, *29*, 1460−1463.
(52) Carrell, C. J.; Carrell, H. L.; Erlebacher, J.; Glusker, J. P. *J. Am. Chem. Soc.* **1988**, *110*, 8651−8656.
(53) Deerfield, D. W., II; Fox, D. J.; Head-Gordon, M.; Hiskey, R. G.; Pedersen, L. G. *Proteins* **1995**, *21*, 244−255.
(54) Sillen, L. G.; Martell, A. E. *Stability Constants*; The Chemical Society: London, 1964; Special Publication No. 17.

$$Mn[H_2O]_6^{2+} \rightarrow Mn[H_2O]_5^{2+}\cdot[OH^-] + H^+ \quad (1)$$

$$Mn[H_2O]_4\cdot[NH_3]_2^{2+} \rightarrow Mn[H_2O]_3^{2+}\cdot[OH^-]\cdot[NH_3]_2 + H^+ \quad (2)$$

$$\text{or} \quad Mn[H_2O]_5^{2+}\cdot[HCO_2^-] \rightarrow Mn[H_2O]_4^{2+}\cdot[OH^-]\cdot[HCO_2^-] + H^+.[3] \quad (3)$$

In the second, a proton is transferred from one of the manganese-bound water molecules to a free water molecule, giving the hydronium ion; i.e., one of the following proton-transfer reactions takes place:

$$Mn[H_2O]_6^{2+} + H_2O \rightarrow Mn[H_2O]_5^{2+}\cdot[OH^-] + H_3O^+ \quad (4)$$

$$Mn[H_2O]_4^{2+}\cdot[NH_3]_2 + H_2O \rightarrow Mn[H_2O]_3^{2+}\cdot[OH^-]\cdot[NH_3]_2 + H_3O^+ \quad (5)$$

$$\text{or} \quad Mn[H_2O]_5^{2+}\cdot[HCO_2^-] + H_2O \rightarrow Mn[H_2O]_4^{2+}\cdot[OH^-]\cdot[HCO_2^-] + H_3O^+ \quad (6)$$

(Unimolecular reactions of the form $M[H_2O]_2^{2+} \rightarrow M[OH]^+ + H_3O^+$ and $M[H_2O]_2^{2+} \rightarrow M[H_2O]^{2+} + H_2O$ have recently been studied by Beyer et al. for M = Be, Mg, Ca, Sr, and Ba using DFT with the large 6-311G(3df,2pd) basis set.[55]) In Table 11, we list the values of ΔH°_{298} and ΔG°_{298} for the deprotonation reactions 1−3. Since there are no experimental energy data available for these processes, we also list in this table the calculated enthalpy and free energy changes for the deprotonation of an isolated water molecule at 298 K using the same computational level. The calculated value of ΔH°_{298}, 389.4 kcal/mol, is in excellent agreement with the experimental gas-phase measurements, which give a deprotonation enthalpy of 391 kcal/mol.[56] The results for the corresponding magnesium complexes are also given in this table.

As can be seen from Table 11, the values of ΔH°_{298} and ΔG°_{298} for the deprotonation of a water molecule in the complexes $M[H_2O]_6^{2+}$ and $M[H_2O]_4^{2+}\cdot[NH_3]_2$ (M = Mn, Mg) are very similar. It requires about 60% less energy to deprotonate one of the water molecules in the inner hydration sphere of a divalent manganese or magnesium ion than it requires to deprotonate an isolated water molecule; the deprotonation enthalpy of $Zn[H_2O]_6^{2+}$ is about 10 and 13 kcal/mol less endothermic than that for $Mg[H_2O]_6^{2+}$ and $Mn[H_2O]_6^{2+}$, respectively. The calculated values of ΔG°_{298} for these direct deprotonation processes, however, are very high. In Table 12, we list the calculated values of ΔH°_{298} and ΔG°_{298} for the corresponding proton-transfer processes, reactions 4 and 5. The analogous reaction involving two isolated water molecules, $2H_2O \rightarrow OH^- + H_3O^+$, is well known to be highly endothermic, the calculated value of ΔH°_{298} being approximately 225 kcal/mol at the MP2(FULL)/6-311++G**//HF/6-31G* computational level.[11] When H_2O is coordinated to divalent manganese or magnesium ions, however, the calculated values of ΔH°_{298} and ΔG°_{298} for reactions 3 and 4 are close to zero, showing that such a proton-transfer reaction is energetically feasible in the gas phase. The corresponding proton-transfer reaction involving $Zn[H_2O]_6^{2+}$ is some 10 kcal/mol exothermic.

The presence of a carboxylate group in the place of a water molecule in the first coordination shell of either manganese or magnesium effectively blocks the proton-transfer reaction in the gas phase. Calculated values of ΔH°_{298} and ΔG°_{298} for the deprotonation and proton-transfer processes involving $Mn[H_2O]_5^{2+}\cdot[HCO_2^-]$ and $Mg[H_2O]_5^{2+}\cdot[HCO_2^-]$ are also given in Tables 11 and 12, respectively, and the results for manganese and magnesium are again found to be nearly identical. There is approximately an 80 kcal/mol *increase* in the endothermicity

Table 11. Enthalpy Changes, ΔH°_{298} (kcal/mol), and Free Energy Changes, ΔG°_{298} (kcal/mol), for Deprotonation Reactions

reaction	metal ion	MP2(FULL)/6-311++G**//HF[a] ΔH°_{298}	MP2(FULL)/6-311++G**//HF[a] ΔG°_{298}
ionization of water:			
$H_2O \rightarrow OH^- + H^+$		+389.4	+382.8
ionization of one water molecule in hexahydrated M^{2+}			
$M[H_2O]_6^{2+} \rightarrow$	Mg	+165.0	+156.3
$M[H_2O]_5^{2+}\cdot[OH^-] + H^+$	Mn	+167.7	+159.7
	Zn	+154.6	+146.4
ionization of one water molecule when two waters in the hexahydrate are replaced by ammonia			
$M[H_2O]_4^{2+}\cdot[NH_3]_2 \rightarrow$	Mg	+166.3	+160.8
$M[H_2O]_3^{2+}\cdot[OH^-]\cdot[NH_3]_2 + H^+$	Mn	+167.3	+161.6
	Zn	+151.4[c]	+147.6[c]
ionization of one water molecule when one water of the hexahydrate is replaced by a carboxylate			
$M[H_2O]_5^{2+}\cdot[HCO_2^-] \rightarrow$	Mg	+246.1	+239.2
$M[H_2O]_4^{2+}\cdot[OH^-]\cdot[HCO_2^-] + H^+$	Mn	+247.0	+239.9
ionization of one water molecule when one water of the hexahydrate is replaced by chloride			
$M[H_2O]_5^{2+}\cdot[Cl^-] \rightarrow$	Mg	+243.1	+237.4
$M[H_2O]_4^{2+}\cdot[OH^-]\cdot[Cl^-] + H^+$		(+245.5)[b]	(+239.8)[b]
	Mn	+239.7	+235.0

[a] HF = HF/6-31G* for the magnesium complexes and HF/HUZ* for the manganese complexes. The thermal corrections and entropies used for the calculation of ΔH°_{298} and ΔG°_{298} are given in Table 5S (Supporting Information) or in refs 10 and 11. [b] The lowest energy form of $Mg[H_2O]_4\cdot[OH^-]\cdot[Cl^-]$ is similar in structure to that shown for manganese in Figure 4. A second-higher-energy form is shown in refs 10 and 11; such a form is apparently not a local minimum on the PES for $Mn[H_2O]_4^{2+}\cdot[OH^-]\cdot[Cl^-]$. [c] One of the water molecules migrated to the second shell of $Zn[H_2O]_3^{2+}\cdot[OH^-]\cdot[NH_3]_2$ during the optimization.

Table 12. Enthalpy Changes, ΔH°_{298} (kcal/mol), and Free Energy Changes, ΔG°_{298} (kcal/mol), for Proton-Transfer Reactions

reaction	metal ion	MP2(FULL)/6-311++G**//HF[a] ΔH°_{298}	MP2(FULL)/6-311++G**//HF[a] ΔG°_{298}
$H_2O + H_2O \rightarrow OH^- + H_3O^+$		+224.6	+225.5
$M[H_2O]_6^{2+} + H_2O \rightarrow$	Mg	+0.1	−1.8
$M[H_2O]_5^{2+}\cdot[OH^-] + H_3O^+$	Mn	+2.9	+1.7
	Zn	−10.2[c]	−11.6[c]
$M[H_2O]_4^{2+}\cdot[NH_3]_2 + H_2O \rightarrow$	Mg	+1.5	+2.8
$M[H_2O]_3^{2+}\cdot[OH^-]\cdot[NH_3]_2 + H_3O^+$	Mn	+2.6	+3.6
	Zn	−13.4[b]	−10.4[b]
$M[H_2O]_5^{2+}\cdot[HCO_2^-] + H_2O \rightarrow$	Mg	+81.3	+81.8
$M[H_2O]_4^{2+}\cdot[OH^-]\cdot[HCO_2^-] + H_3O^+$	Mn	+82.2	+81.8

[a] HF/6-31G* for the magnesium complexes and HF/HUZ* for the manganese complexes. The thermal corrections and entropies for the calculation of ΔH°_{298} and ΔG°_{298} are given in Table 5S (Supporting Information) or in refs 10 and 11. [b] One of the water molecules migrated to the second shell of $Zn[H_2O]_3^{2+}\cdot OH^-\cdot[NH_3]_2$ during the optimization; i.e., the inner coordination number of $Zn[H_2O]_3^{2+}\cdot OH^-\cdot 2NH_3$ is 5.[c] At the HF/HUZ* computational level, the coordination number of $Zn[H_2O]_5^{2+}\cdot[OH^-]$ is 6.

(55) Beyer, M.; Williams, E. R.; Bondybey, V. E. *J. Am. Chem. Soc.* **1999**, *121*, 1565−1573.

(56) Bartmess, J. E.; McIver, R. T., Jr. In *Gas-Phase Ion Chemistry*; Bowes, M. T., Ed.; Academic Press: New York, 1979; Vol. 2, pp 87−121.

Table 13. Enthalpy Changes, ΔH°_{298} (kcal/mol), and Free Energy Changes, ΔG°_{298} (kcal/mol), for Water Dissociation Reactions

		MP2(FULL)/6-311++G**//HF[a]	
reaction	metal	ΔH°_{298}	ΔG°_{298}
$M[H_2O]_6^{2+} \rightarrow M[H_2O]_5^{2+} + H_2O$[b] (CN = 6) (CN = 5)	Mg	+31.9	+19.3
	Mn	+28.7	+17.1
	Zn	+27.1	+15.4
$M[H_2O]_5^{2+}\cdot[HCO_2^-] \rightarrow M[H_2O]_4^{2+}\cdot[HCO_2^-] + H_2O$ (monodentate) (CN = 6) (bidentate) (CN = 6)	Mg	+16.7	+5.7
	Mn	+16.3	+5.4

[a] HF/6-31G* for the magnesium complexes and HF/HUZ* for the manganese complexes. [b] For comparison, the dissociation enthalpies for $M[H_2O]^{2+}$ (M = Mg, Mn) are +76.8 and +75.7 kcal/mol, respectively, at the CCSD(T)(FULL)/MP2(FULL)/6-311++G** computational level.[39]

of these processes compared to those for the corresponding hexahydrates. This is consistent with the results of Bertini et al.,[51] who reported an 82 kcal/mol increase in the energy required to deprotonate $Zn[NH_3]_2^{2+}\cdot[HCO_2^-]\cdot[H_2O]$ compared to $Zn[NH_3]_3^{2+}\cdot[H_2O]$. In considering the deprotonation of $Zn[H_2O]_4^{2+}\cdot[NH_3]_2$, the HF/HUZ* optimization of the hydroxide $Zn[H_2O]_3^{2+}\cdot[OH^-]\cdot[NH_3]_2$, which had an initial geometry with CN = 6, led to a structure with CN = 5, where one of the water molecules moved to the second hydration shell; a second water molecule involved a long Zn···O bond distance, 2.415 Å. To evaluate whether this was a result of the computational level that we employed, the $Zn[H_2O]_3^{2+}\cdot[OH^-]\cdot[NH_3]_2$ complex was reoptimized using DFT at the B3LYP/6-311++G** level. This optimization also resulted in a structure with one of the water molecules in the second shell (bridging the two NH_3 groups); the other water molecule was found to be 2.891 Å from the zinc ion, suggesting an inner-shell coordination number of 4. Interestingly, reoptimizing $Zn[H_2O]_5^{2+}\cdot[OH^-]$ at the B3LYP/6-311++G** level resulted in a structure with CN = 5, where one water molecule migrated to the second shell during the optimization. It should be noted that reoptimizing the corresponding magnesium(II) complexes at this level did not result in a coordination number change.

To a large extent, the increase in the enthalpy required for the deprotonation of (or proton transfer from) the carboxylate-containing complexes is a direct result of the reduced net charge on the complex. This was demonstrated by calculating the deprotonation enthalpy for the $Mn[H_2O]_5^{2+}\cdot[Cl^-]$ (see structure **16** in Figure 4), which has a chloride ion in place of the carboxylate group; the corresponding hydroxide is shown as structure **17**. The values of ΔH°_{298} and ΔG°_{298} for the deprotonation are listed in Table 11, along with the corresponding results for $Mg[H_2O]_5^{2+}\cdot[Cl^-]$. Although more charge (nearly 0.1e at the MP2(FULL)/6-311++G**//HF/HUZ* level, see Table 3S, Supporting Information) is transferred to the manganese ion from the ligands in $Mn[H_2O]_5^{2+}\cdot[Cl^-]$ than in $Mn[H_2O]_5^{2+}\cdot[HCO_2^-]$, the values of ΔH°_{298} (and ΔG°_{298}) for the deprotonations are very similar. Thus, the net charge on the complex plays a dominant role in the energetics of these protonation and proton-transfer reactions, while small differences in the charge or electron configuration on the divalent manganese or magnesium ion play a relatively minor role.

c. Dehydration of $Mn[H_2O]_6^{2+}$ and $Mn[H_2O]_5^{2+}\cdot[HCO_2^-]$. The structures of $Mn[H_2O]_5^{2+}$ (**18**) and $Mn[H_2O]_4^{2+}\cdot[HCO_2^-]$ (**19**; bidentate formate) are shown in Figure 4. In Table 13, we compare the energy requirements for removing one water molecule from $Mn[H_2O]_6^{2+}$, where the corresponding results for magnesium and zinc are also given. The values of ΔG°_{298} for these dehydration reactions are all positive and decrease from Mg^{2+} to Mn^{2+} to Zn^{2+}. Our calculated value of ΔH°_{298} for the removal of a water molecule from $Mg[H_2O]_6^{2+}$ to give $Mg[H_2O]_5^{2+}$, 31.9 kcal/mol, is in reasonable agreement with that of Glendening et al.,[57] 29.2 kcal/mol, but slightly higher than that found from the B3LYP/LANL2DZ calculations of Pavlov et al.,[31] 24.5 kcal/mol. An experimental value of 24.6 kcal/mol was recently obtained by Peschke et al.[58] from high-pressure mass spectrometry equilibrium experiments. Blackbody infrared radiative dissociation experiments indicate that, at low temperatures, the structure of the hexahydrated divalent magnesium is $Mg[H_2O]_6^{2+}$, although at higher temperatures the structure is proposed to be $Mg[H_2O]_4^{2+}\cdot[H_2O]_2$.[33,34] Furthermore, the preferred structure for pentahydrated Mg^{2+} is apparently $Mg[H_2O]_4^{2+}\cdot[H_2O]$[33,34] at higher temperatures rather than $Mg[H_2O]_5^{2+}$. Experimental data for the corresponding manganese complexes are not yet available.

When one inner-sphere water molecule is replaced by a carboxylate group, the values of ΔG°_{298} for the dehydration of $M[H_2O]_5^{2+}\cdot[HCO_2^-]$ are smaller than those for the hexahydrates. This is partly due to the fact that the optimized structure of $M[H_2O]_4^{2+}\cdot[HCO_2^-]$ is bidentate for both Mg^{2+} and Mn^{2+}, thus conserving a coordination number of 6 in the reaction and illustrating the preference of these ions for hexacoordination.

Discussion and Conclusions

a. General Geometries of Mn^{2+} Complexes Compared with Those of Some Other Divalent Cations. Our analysis of ligand composition for divalent manganese has shown that Mn^{2+} has coordination preferences similar to those of Mg^{2+} (see Figure 1); this is in keeping with its somewhat "softer" characteristics but is quite distinct from Zn^{2+}, which is considerably softer (more polarizable) than either Mg^{2+} or Mn^{2+}. Our calculations give results in agreement with these observed binding preferences. Mn^{2+} is slightly larger in size (by about 0.1 Å) than Mg^{2+}, but its binding is similar. Calcium, on the other hand, is considerably larger than Mg^{2+}, Mn^{2+}, or Zn^{2+}, and it binds almost exclusively to oxygen in ligands. Results from crystal structure analyses indicate that the predominant first-sphere coordination number is 6 for both Mn^{2+} and Mg^{2+}, while for Zn^{2+} coordination numbers 4, 5, and 6 are all common, as are 6, 7, and 8 for Ca^{2+}. These results are diagrammed in Figure 2. Mn^{2+} does not show the strong tendency of Mg^{2+} to bind six water molecules to give $M[H_2O]_6^{2+}$ (found in crystal structures). In the Mn^{2+} complexes, water in the inner sphere is more readily replaced by other groups than it is in the corresponding Mg^{2+} complexes. Our computational results show that, in the hexahydrates, the metal−oxygen bonding is mainly electrostatic in nature. Although a small amount of charge (0.31e) is transferred to Mn^{2+} from inner-sphere water, this is less than that for Mg^{2+} (0.20e).

(57) Glendening, E. D.; Feller, D. *J. Phys. Chem.* **1996**, *100*, 4790−4797.

(58) Peschke, M.; Blades, A. T.; Kebarle, P. *J. Phys. Chem. A* **1998**, *102*, 9978−9985.

One distinction between Mn^{2+} and Mg^{2+} is that Mn^{2+} often binds carboxylate groups in a bidentate manner, in contrast to Mg^{2+}, which does not show this tendency. This may be a result of the sizes of the two cations, since the space occupied by a carboxylate group (with O···O approximately 2.2 Å) is less than that required by water molecules (with O···O approximately 2.7 Å). The surface area of a sphere at the Mg^{2+}···O distance of 2.07 Å is 53.8 Å^2, corresponding to about 9 Å^2 per water molecule in the hexahydrate. The corresponding area for Mn^{2+} is 59.2 Å^2, an increase of 5.4 Å^2, somewhat more than half the space occupied by a water molecule. This extra area can be filled with a smaller ligand or by bidentate coordination of a carboxylate group. Similar arguments that were applied to Ca^{2+} (Ca^{2+}···O = 2.42 Å, giving an area for a sphere at that distance from Ca^{2+} of 73.6 Å^2) are consistent with coordination of 8.2 water molecules.

b. Effects of Changing the Number and Types of Ligands in the Inner Coordination Sphere. The energy penalties for changing a hexaaquated metal cation, $M[H_2O]_6^{2+}$, with six water molecules in the innermost coordination sphere to one with five water molecules in the inner sphere and one in the second sphere or four in the inner sphere and two in the second sphere of these divalent cations were investigated. The penalty for Mn^{2+} is intermediate between that for Mg^{2+} (which is high) and Zn^{2+} (which is low). The very low barrier that some Zn^{2+} complexes have with respect to coordination number alteration can have important structural consequences, even in the case of the simple gas-phase complexes we have described. Ca^{2+}, which is larger, shows a low penalty for changes between inner-shell coordination numbers of 6, 7, and 8.

The binding propensities of metal ions with respect to the three possible ligand atoms (O, N, S) found naturally in proteins are highlighted by triangular plots of binding as a function of inner coordination number in Figure 2. A remarkable similarity of Mn^{2+} to Mg^{2+} at coordination numbers 6 and 7 is shown here. The main difference is the larger probability for nitrogen as a ligand for $Mn^{2+}$and the higher tendency of Mn^{2+} to bind sulfur at lower coordination numbers, similar to that for zinc. Calcium, on the other hand, mainly binds oxygen ligands at each coordination number.

A variety of Mn^{2+} complexes were studied by ab initio molecular orbital and DFT calculations. We find that more negative charge is transferred to the 3s or 4s orbitals of the metal ion from ligand as it is changed from O to N to S, the transfer being greater for the more polarizable Mn^{2+} than for Mg^{2+}. The relative affinities of Mn^{2+} and Mg^{2+} ions for nitrogen- and oxygen-containing ligands to give hexacoordinated cations were assessed from calculated enthalpy and free energy changes on transfer. These confirm that Mn^{2+} has a somewhat higher affinity for nitrogen than does Mg^{2+} (which prefers oxygen). This is also reflected in the presence of nitrogen ligands to the metal ion in natural manganese proteins.

c. Effects on the Reactivity of Metal Ion-Bound Water. The enthalpy change for removing a water molecule from $M[H_2O]_6^{2+}$ or removing a carboxylate group from $M[H_2O]_5^{2+}\cdot[HCO_2^-]$ is slightly less for Mn than for Mg, confirming that magnesium binds water more strongly than does divalent manganese. This is reflected in the exchange rates of water in the inner coordination sphere (6×10^5 s^{-1} for Mg^{2+}, 2×10^7 s^{-1} for Mn^{2+} and Zn^{2+}, and 3×10^8 s^{-1} for Ca^{2+}).[59,60]

The binding of a water molecule to a metal ion facilitates its ionization to hydrogen ions and hydroxyl ions. Three reactions of metal ion-bound water have been identified for $M[H_2O]^{2+}$ (M = Mg, Ca, Sr, Ba).[55] They are proton transfer to give MOH^+ and H_3O^+, water loss to give $M[H_2O]^{2+} + H_2O$, and charge transfer to give H_2O^+ and $M[H_2O]^+$. The last of these three is generally not favorable. We found the enthalpy change for the deprotonation (or proton transfer) of $M[H_2O]_6^{2+}$ or $M[H_2O]_5^{2+}$ to be slightly greater for M = Mn than for M = Mg or Zn. Energies for deprotonation of a water molecule in $M[H_2O]_6^{2+}$ and $M[H_2O]_4^{2+}\cdot[NH_3]_2$ (M = Mg, Mn) are very similar, so that replacing oxygen by nitrogen in the inner coordination sphere does not cause significant changes in reactivity. Our deprotonation results suggest that Mn^{2+} does not polarize water as well as Mg^{2+} or Zn^{2+}. Calculations on the monohydrates $M[H_2O]^{2+}$ (where M = Mg and M = Ca to Zn in the Periodic Table) indicate that replacing Mg by Mn generally alters the binding enthalpies and charge distribution of these monohydrates to a lesser extent than does using the other metal ions in the sequence Ca to Zn.[30] We have shown that replacement of an inner-shell metal ion-bound water molecule by an anionic ligand, such as a carboxylate group, effectively blocks the ability of either Mn^{2+} or Mg^{2+} to facilitate ionization of water by an electrostatic effect. Based on the ionic radii of Mg^{2+}, Mn^{2+}, and Zn^{2+} and the metal ion−oxygen distances in hexahydrated complexes, one might have expected Zn^{2+} to be a better replacement than Mn^{2+} for Mg^{2+}, but experimentally this is not the case. This may reflect the greater coordination flexibility in complexes containing Zn^{2+} compared to those containing Mn^{2+}, and it suggests that size and charge are not the sole determinants of metal ion specificity in proteins.

We have found that divalent manganese will bind more readily to a site containing nitrogen in addition to oxygen than will Mg^{2+}, which prefers oxygen only. Therefore, we examined crystal structures of Mn^{2+}-containing enzymes in the PDB. While some are naturally occurring Mn^{2+}-binding enzymes, others were made with Mn^{2+} as a replacement for Mg^{2+} in order to aid in crystal structure determination. With this reservation in mind, we found that, in a sample of 18 crystal structures containing 24 Mn^{2+} sites in all, 11% of the ligands to Mn^{2+} were nitrogen (mainly histidine, one lysine). This is in contrast to the ligands to Mg^{2+} in proteins, which are nearly always oxygen. In addition, Mn^{2+} binding was found to involve 31% Asp or Glu, 17% phosphate, and 31% water in the 18 structures we selected at random. There appeared to be a motif consisting of His, Glu, two Asp, and two water molecules bound to Mn^{2+}. Thus, an enzyme acquires control over the binding of Mg^{2+} versus Mn^{2+} (or other nitrogen-binding ligands) by inserting a nitrogen-containing ligand in the site that should exclude Mg^{2+} but bind Mn^{2+}. While this is not a precise discrimination, enzyme crystal structures, such as that of *Escherichia coli* phosphoenolpyruvate carboxykinase,[61] provide experimental evidence for this suggestion.

Acknowledgment. We thank the Advanced Scientific Computing Laboratory, NCI-FCRF, for providing time on the CRAY supercomputers, and Carol Afshar for technical assistance. This work was supported by Grants CA10925, CA06927, and GM31186 from the National Institutes of Health and by an appropriation from the Commonwealth of Pennsylvania. Its contents are solely the responsibility of the authors and do not necessarily represent the official views of the National Cancer Institute.

(59) Frey, C. M.; Stuehr, J. In *Metal Ions in Biological Systems*; Sigel, H., Ed.; Marcel Dekker: New York, 1974; Vol. 1, p 69.

(60) Ducommum, Y.; Merbach, A. E. In *Inorganic High-Pressure Chemistry*; van Eldik, R., Ed.; Elsevier: Amsterdam, 1986.

(61) Tari, L. W.; Matte, A.; Goldie, H.; Delbaere, L. T. J. *Nature Struct. Biol.* **1997**, *4*, 990−994.

Supporting Information Available: Table 1S, listing 542 divalent manganese-containing crystal structure and refcodes (from the CSD) as a function of coordination number; Table 2S, giving ligand identities with corresponding refcodes; Table 3S, listing NPA charges and natural electron configurations for selected manganese and magnesium complexes; Table 4S, comparing the M−O distances (Å), binding enthalpies, ΔH°_{298} (kcal/mol), and charges for the divalent metal monohydrates $Mg^{2+}[H_2O]$ and $M^{2+}[H_2O]$ (M = Ca, Cr, Mn, Fe, Co, Ni, Cu, and Zn);[30] Table 5S, listing calculated atomic coordinates, *X*, *Y*, and *Z*, of the various manganese complexes: Table 6S, giving total molecular energies (au), entropies (cal/mol-K), and thermal corrections (kcal/mol) for the divalent manganese complexes; and Figure 1S, showing detailed structures **4**−**19** from calculations showing bond lengths (in Å), interbond angles (in degrees), and net atomic charges (NPA analysis) [no parentheses, HF/HUZ*//HF/HUZ*; < >, HF/6-311++G**//HF/6-31++G**; and ( ), MP2(FULL)/HUZ*//MP2(FULL)/HUZ*] (PDF). This material is available free of charge via the Internet at http://pubs.acs.org.

JA9906960